As can be seen from these graphs the degree of polarization of the scattered wave depends on the order of scattering. Thus, every wave becomes partially depolarized on each phase screen at each scattering act. So if the number of screens is increasing ($n \to \infty$) that the depolarization to tend to a limit which of equal to 100%.

Conclusions. The mathematical model of light propagation through media with multiple scattering which was based on the approximation by sequence of the anisotropic phase screens. It has been considered case of the stratified medium, in which anisotropy is sequent of statistical inhomogeneous of the layers interfaces. The essential depolarization effect at the light propagation has been confirmed experimentally. This fact was submitted to theoretical results which obtained from proposed model.

Reference

1. Goodman G.W. Statistical optics /G.W.Goodman. John Wiley and Sons: New York-Chichester-Brisbane-Toronto-Singapore, 1985. – 487p. 2. Alloin D. M. Adaptive Optics for Astronomy / D. M. Alloin, J.-M. Mariotti. NATO ASI Series: Kluwer Academic Publ., 1994. – .423 p. 3. Azzam R.M.A. Ellipsometry and polarized light. 5th ed./ R.M.A.Azzam, N.M.Bashara. Elsevier: North Holland. 2003. – 387p. 4. Andrews L.S. Propagation of a Gaussian-beam wave through a random phase screen/ L.S.Andrews, R.L.Phillips, A.R.Weeks// J. Waves Random Media. – 1997. – Vol. 7. – P.229–244. 5. Barchuk O.I. Experimental investigations of light depolarization under multiple scattering / O.I.Barchuk, A.A.Goloborodko, V.N.Kurashov, Y.A. Oberemok, S.N. Savenkov // Proceedings of SPIE. – 2006. – Vol.6254 – 62540W. 6. Дерюгина А.И. Поляризационная структура дифрагованого излучения, распространяющегося в турбулентной атмосфере / А.И. Дерюгина, В.Н. Курашов, А.И. Мащенко // Радиотехника и электроника. – 1988. – Том 23, №11 – С. 2399–2408. 7. Kurashov V.N. Polarization changes in coherent electromagnetic radiation scattering by the rough surface/ V.N. Kurashov, V.V. Marienko, T.V. Molebna, A.G.Chumakov // Proceedings of SPIE. – 1995. – Vol. 2647. – P. 48–56.

Submitted on 19.10.12

А. Голобородько, канд. фіз.-мат. наук, каф. нанофізики та наноелектроніки, радіофізичний факультет, КНУ імені Тараса Шевченка, Київ

РОЗПОВСЮДЖЕННЯ КОГЕРЕНТНОГО ВИПРОМІНЮВАННЯ В ОПТИЧНО НЕОДНОРІДНОМУ СЕРЕДОВИЩІ

Проведено теоретичний аналіз явища деполяризації оптичних сигналів, що розповсюджуються оптичним середовищем зі статистично розподіленими параметрами. Дослідження поляризаційних характеристик випромінювання виконано з використанням методу кореляційної матриці. Розглянуті поляризаційні властивості оптичних полів, що сформовані в зоні дифракції Фраунгофера.

Ключові слова: ступінь поляризації, статистично неоднорідне середовище.

А. Голобородько , канд. физ.-мат. наук, каф. нанофизики и наноэлектроники радиофизический факультет, КНУ имени Тараса Шевченко, Киев

РАСПРОСТРАНЕНИЕ КОГЕРЕНТНОГО ИЗЛУЧЕНИЯ В ОПТИЧЕСКИ НЕОДНОРОДНОЙ СРЕДЕ

Проведен теоретический анализ явления деполяризации оптических сигналов, распространяющихся в оптической среде со статистически распределенными параметрами. Исследование поляризационных характеристик излучения выполнены с использованием метода корреляционной матрицы. Рассмотрены поляризационные свойства оптических полей, сформированных в зоне дифракции Фраунгофера.

Ключевые слова : степень поляризации, статистически неоднородная среда.

UDC 576.535; 577.151.45; 577.037; 577.325.5

O. Ivanyuta, Ph.D.
Department Electrophysics, Faculty of Radiophysics,
Taras Shevchenko National University of Kyiv

ELECTROPHYSICS PROPERTIES THE DNA AND DNA:AU MOLECULAR CLUSTERS ON SAPPHIRE

The films DNA, DNA: Au, clusters from gel solution, which can be magnetic and electrical active in biosensor systems and to detect their functional properties by microwave techniques. Research has been focused on the application of I - V characteristics and spectra methods to recognise and predict these molecular interactions based on primary structure and associated physic-chemical properties. In results have actually shown that these molecular cluster layers on Al_2O_3 substrates can to conduct electric current and respond on power of microwave.

Keywords: DNA, UV-VIS-NIR spectra, low-energy electron point source, current-voltage characteristics.

Introduction. Deoxyribonucleic acid (*DNA*) encodes the architecture and function of living cells. DNA is made of a sequence of four bases: adenine (*A*), guanine (*G*), thymine (*T*) and cytosine (*C*) (Fig. 1), attached to a phosphate-sugar backbone and is about 0,34 nm long. Any particular sequence forms a single strand of *DNA*. Two strands may come together through hydrogen bonding of the bases *A* with *T* (*A T*) and *G* with *C* (*GC*) [1–4].

DNA's electronic and self-assembly properties bear enormous importance in nanoscience. The electrophysics properties *DNA* are interest in several disciplines in nanoscience because of their relevance to damage and mutation in molecules. The charge transport for electrophysics properties of *DNA* is central to such developments. For instance, electrophysics detection of structural changes, due to protein binding or base mismatches examined. New read-out schemes on *DNA* chips can detect for the presence of different *DNA* sequences, might exploit her a electronic properties. The phosphate ion carries a negative charge in the *DNA* molecule, which results in electrostatic repulsion of the two strands. In order to keep the two strands together, positive ions must be present in the solution to keep the negative charges neutralized. Charge transport in *DNA* can shed new light on the transport properties of other systems with supramolecules (Fig. 2). *DNA* could be a *Au* conductor because of the formation of a molecules band across the different bases. The stacking molecule is important in the conducting properties of several other organic molecules, that DNA might conduct started to be pursued with more vigor. The electron transfer through *DNA* was responsible for fluorescence quenching of an excited molecule [2–5, 9, 10].

DNA behaves as a conductor, semiconductor, or insulator, in what seems to be contradictory conclusions. The apparent contradictions have been attributed to the large phase space in which *DNA* can be prepared and probed. Many experimental conditions and attributes of the specific *DNA* used, including base sequence, length, orientation, countering, temperature, electrode contact, adsorption surface, fluctuations, and so on, could affect its conducting properties. As a consequence, although much

progress has been made, *DNA*'s transport properties are still in question. The electrophysics properties free metal (*Au*) clusters sensitively depend on the exact number atoms *N* in island films to study the influence of a supporting or embedding medium on the electronic level structure. The island film for conserving the distinct energy spacing's of a deposited cluster, it would be possible to generate a clusters with adjustable electronic and optical properties. The size cluster determines surface reactivity film. As illustrated in Fig. 3, this method involved attaching noncomplementary *DNA* oligonucleotides to the surfaces of two batches of *Au* particles capped with thiol groups, which bind to gold (see Fig. 2). The presence a surface will significantly influence the electronic level structure in the cluster at a large distance the only common energy is the vacuum energy, E_{vac}. As the temperature is reduced, the two strands will eventually come together by diffusion and rehybridize to form the double stranded structure. These properties of the *DNA* can be utilized in the ordering and assembly of artificial structures if these structures can be attached to *DNA* [4–6, 9, 10].

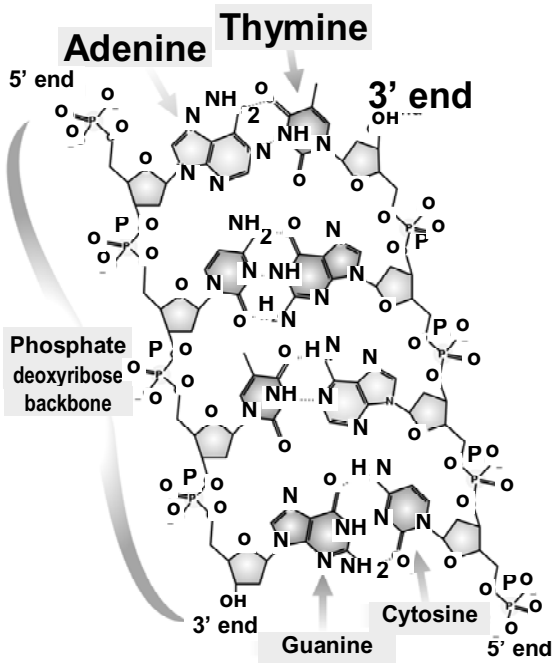

Fig. 1. Chemical structure of DNA (from Wikipedia)

Results and discussion. Direct measurements *DNA* in vacuum are showed good conduct properties. It was found that *DNA* is a conductor, with a resistance comparable to that of conducting polymers. So far, the most widely used attachment scheme utilizes the covalent bond between *DNA* and *Au*. The experiment was done in gel, where a drop of solution containing *DNA – Au* was placed onto sapphire with a foil gold-covered with $3\ \mu m$.

The DNA ropes were then broken by using a tungsten tip. The tip was also used to apply a bias across the DNA. A $600\ nm$ portion of a *DNA* rope produced a resistance of the electrodes in series with a resistor $R = 100\ k\Omega$ or $1\ M\Omega$. At low bias voltages, no current is measured, $2{,}5\ M\Omega$ [4, 10]. The experiments were done using a *DNA* oligomer 250 base pairs $56{,}2\ nm$ long. An electrostatically trapping technique was used to position single *DNA* molecules between two electrodes $10\ nm$ apart (see Fig. 3). Electrical contacts between *DNA* molecules and Au electrodes were made by using the electrostatic trapping method [4, 12]. *DNA* was researched with a low-energy electron point source (LEEPS) microscope with not radioactively damage *DNA*. [4–5].

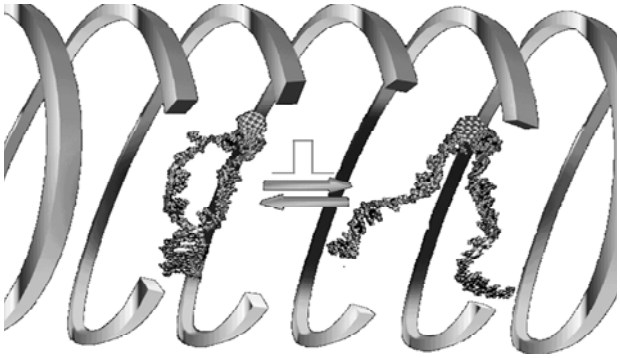

Fig. 2. DNA/*Au* nanoparticles as building blocks formation

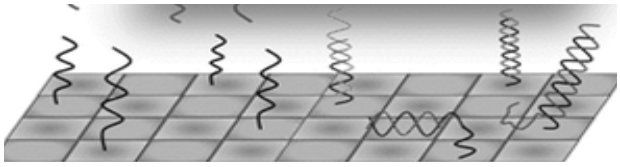

Fig. 3. Size cluster was 3 μm and determines surface reactivity film

When two oligonucleotides which are complementary to the two grafted sequences are introduced, the nanoparticles self-assemble into aggregates. This process could also be reversed when the temperature was increased due to the melting of the *DNA* oligonucleotides. Because of the molecular recognition properties associated with the *DNA* interconnects, this strategy allows one to control interparticle distance, strength of the particle interconnects, and size and chemical identity of the particles in the targeted macroscopic structure. The sample was then dried with a flow of nitrogen. The current (I) – voltage (U) characteristics are measured using the equipment, which is the same to the *LEEPS*. Sensitivity the measurement of current is $10\ pA$. The time was to writing of the characteristic under the change of the voltage from $-10\ V$ to $+10\ V$ with step $10\ mV$ for 100 seconds. The measurement was made in air at $T = 300\ K$. This provides an upper value for the resistance of DNA, since some finite contact resistance is expected to contribute. Since the experiment was done in vacuum, ionic conduction could not account for the transfer mechanism. However, this experiment does not rule out that ions trapped by the *DNA* might have changed its electronic structure, allowing for higher conductivity. There has also been some evidence that *LEEPS* imaging contaminates the *DNA* and can account for the conducting behavior observed in this experiment. The visible absorption spectra of these gels in quartz cuvetes were recorded on *UV – VIS* spectrophotometer with double-beam mode through CDD (cooled double detection) Specord 200, Analytik Jena AG. The transmission spectra Au / *DNA* nanosystems was in 2D - plates and *DNA* molecule in adsorbed layers from gels on dielectric substrate. *IR* spectra of the adsorbed layers from these gels on dielectric substrate KRS - 5 were recorded using a Bruker IFS 66v spectrometer in the range of $800 \div 1500\ cm^{-1}$ at $T = 300\ K$ [2–4, 9–13].

In other direct measurements have found that DNA acts as a large bandgap semiconductor. With decreasing separation the energy barrier between cluster and sonde will also decrease. The cluster level structure might change when compared to the corresponding free system. As is

clear from Figure 4 and Figure 5, the *DNA* oligomers does not conduct charge for voltage below about 2 V at room temperature, which shows that the human chromosome Ch 22 behaves like a semiconductor with a large bandgap. This characteristic have following features: a non-linearity and unsymmetrical behavior. The tip is held at 2 V A Coulomb blockade like staircase is observed whose origin is still unclear. Then, a voltage of up to 5 V was applied to while the current rises rapidly above a certain threshold voltage. In addition, a large hysteresis is seen by comparing the upward and the downward sweeps. After trapping *DNA* molecules between electrodes, the sample was dried with a nitrogen gas and characterized using precision microwave parameter analyzers (P1 – 59, P1 – 61, P1 – 67). At a higher bias, the *DNA* becomes conductive. Surprisingly, the $I - V$ characteristics were dependent on the direction of the scan rate, yielding different I - V curves. By depositing more silver and thereby growing a thicker *Au* – *DNA*, the noncurrent region was reduced from 5 V to 0,5 V , demonstrating crude control over the electrical properties of these systems. In addition, control experiments where one of the components (*DNA* or *Au*) was removed from the assembly produced no current, establishing that all of the components are necessary to form the conducting *Au* films [3–6, 10–14].

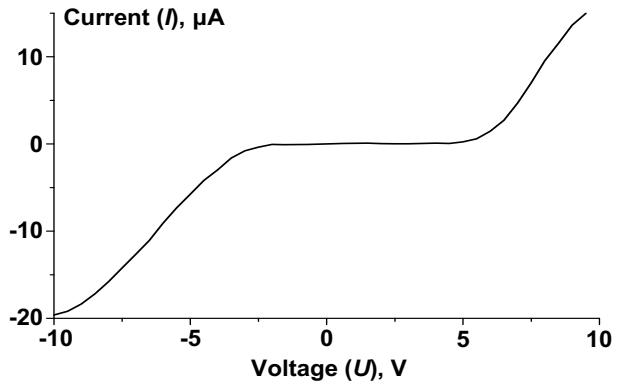

Fig. 4. Current – voltage characteristics of double-strand *DNA* sequence for oligomer 250 base pairs the human chromosome Ch22 [4, 9]

The details of the binding determine whether the highest occupied level in the cluster adjusts to the substrate Fermi energy E_f (Fig. 6). In this case the contact potential would induce a local charge accumulation. Also, the core levels might shift. On a *Au* surface the cluster forms a metallic bond and often likes to wet the substrate sapphire. If the cluster is of the same material as the surface it will form an epitaxial layer. On a non-metallic and weakly interacting surface clusters might keep their identity and have structures close to those of the free clusters in vacuum. The homogeneous sequence is ideal for overlap of π - orbital's in adjacent base pairs. The next part of these features can be conditioned to the electronic structure of these layers and a interface in heterostructures conductance, $(dI/dV)/(V)$ (see Fig. 6), that represents the shape of density of states of *t*. These results do not rule out the possibility that ions could be attached to the DNA, thus modifying its electronic structure. The voltage dependence of the differential conductance as well as normalized conductance exhibits a clear peak structure, which represent a local level of energy that is typical in the polymers *Au* nanoparticles, which have nonmetallic properties. In order to study the electronic structure I investigated the shape of the normalized differential the layer. The different curves show repeated measurements. The telemetric *DNA* sequence, when treated as a quantum wire in the fully coherent low and room temperature regime, works as an excellent semiconductor. Although the origins of voltage gap and hysteresis are not clear, I speculate that the voltage gap and/or the hysteresis are at least partly related to the contacts between electrodes and DNA molecules. In order to study the innocence caused by the contacts, the four probe measurements need to be performed. *G* have peculiar sequence of *H* - bond donor or acceptor groups, and because it has the lowest oxidation potential among the *DNA* bases, which favors self-assembly and carrier transport. Such a *G* in supramolecular assembly has the form of long ribbons, with a strong intrinsic dipole moment along the ribbon axis that causes current rectification in transport experiments. The devices exhibit a maximum voltage gain of 0,79 eV. This approach has potential to express control the size and the packing density of the *Au* nanocrystals by simply adjusting external experimental conditions such as *pH*, temperature, and ion concentration [4, 12–15].

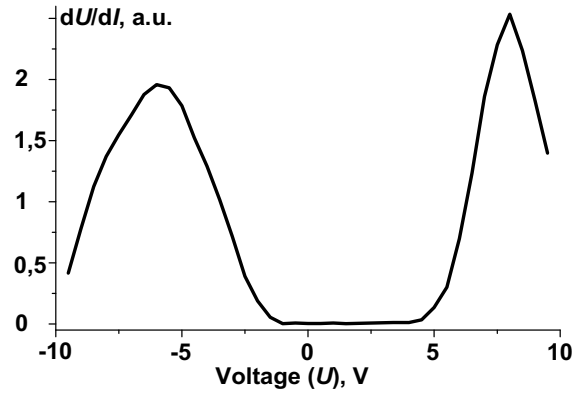

Fig. 5. The differential resistance – voltage characteristics of double-strand *DNA* sequence for oligomer 250 base pairs the human chromosome Ch22

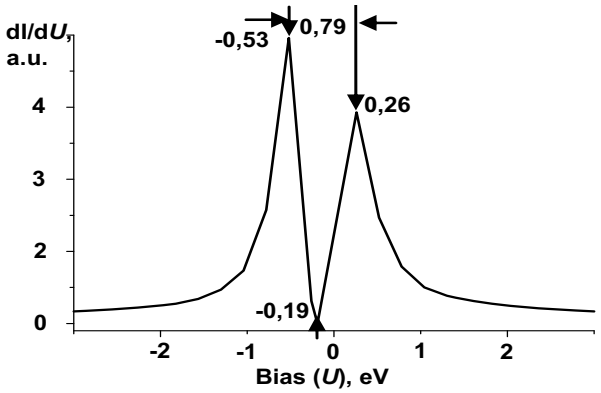

Fig. 6. The differential conductivity – voltage characteristics of double-strand *DNA* sequence for oligomer 250 base pairs the human chromosome *Ch* 22

It can be seen from normalized differential conductance – voltage curves that there is a voltage gap at low applied bias. The value of energy gap for the *Au* clusters was estimated from the range with minimum of DOS near the Fermi level (in Fig. 6. near the point $U = 0$ V). It is turned out that $E_g = 0{,}79$ eV . Using the data of the band gap of *Au* clusters was estimate the cluster diameter: $E_g = 0{,}79$ eV are two dimensional (2*D*) clusters (cluster diameter is approximately 2,4 nm).The change in conductivity due to

the different compressions can be explained as follows: If the charge transport relies on a very organized *DNA* chain, then compression will disrupt the channel conductivity greatly. The compression could be o f such a magnitude that the single strands in the *DNA* duplex are essentially independent. Islands with two layers of gold and a band gap of $0,3 \cdot eV$ are found to be most effective for catalyzing reaction. These results suggest that supported clusters may have unusual catalytic properties as one dimension of the clusters becomes smaller than three atomic spacing's. Its conclude that the observed tailoring of the properties of small *Au* clusters by altering the cluster size and its support could prove to be universal for a variety of metals and will likely be quite useful in the design of nanostructured materials for catalytic applications [6, 13–16].

Ionization potential has electric field difference between two isolated bases ($U_{max} = 0,6$ eV between *G* and *T*). A high *DNA* surface density on the *Au* nanoparticle is expected to provide advantage in particle stabilization the hybridization efficiency. The *dc* impedance spectrum of this gap electrode gives rise to a conductive non large hysteresis with a charge transfer resistance of about $1\ M\Omega$, as shown in the inset of Fig. 7. This resistance (*R*) the layer from *DNA* polymerized molecules versus temperature (*T*) change has exponential decrease at the temperature increase. If it is assumed that there are no other single *DNA* molecules stretched over the gap and this bundle of *DNA* molecules contributes all of the electrical conduction, the resistance of this bundle will be about 10^{-7} cm^{-2}. The rectified type of *I* - *V* characteristic for the structure metal (*Au* or *Ag*) – the layer from *DNA* polymerized molecules networks on sapphire has been confirmed. The spectrum still shows a conductive non large hysteresis with a charge-transfer resistance of $20\ M\Omega$, about 20 seconds times larger than the one measured before the enzyme application.

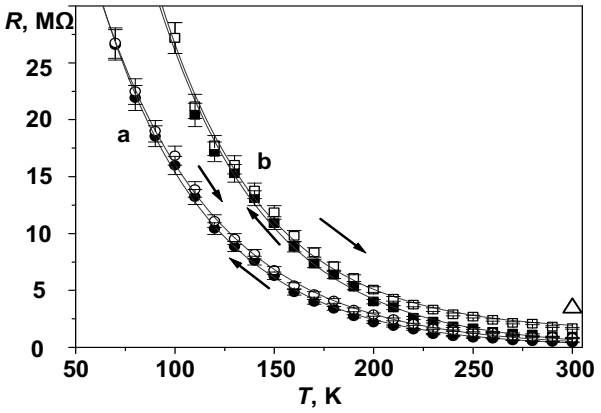

Fig. 7. The resistance (*R*) versus temperature (*T*) curves of the layer from *DNA* polymerized molecules networks on Al_2O_3 (■ and □- points) and on Al_2O_3 after several temperature cycling (×and ◊ points) surfaces (*a* and *b*, respectively). These curves correspond to measurements at one temperature cycling (temperature decreases from 300 K to 70 K and increases from 70 K to 300 K). The value of the resistance of this layer on Al_2O_3 (Δ– point) after temperature cycling is indicated

I cannot degrade all characteristics of double-strand *DNA* sequence for oligomer *A*, *C*, *G*, *T*. After repeated temperature cycling is indicated DNA molecules inside for bundle oligomers 250 base pairs under the applied experimental condition. They fail to respond to changes in the external environment (Δ - point in Fig. 7.) Such behavior of the resistance of the layer from DNA polymerized molecules networks on sapphire under the temperature increase is typical for a semiconductor. Similar results for the layer from *DNA* - linked *Au* nanoparticles in networks have been obtained. But both the resistance of this layer of and its change were less.

However, it should remove all other damaged (stretched) single *DNA* or small bundles of DNA molecules As a result it can be reasonably assumed that this bundle of no degraded *DNA* molecules contributes all of the electrical conduction measured with the *ac* impedance spectroscopy. The resistance is about 10^{-6} cm^{-2} for this *DNA* bundle that may contain about 250 molecules since the diameter for a single *DNA* is about 2,4 nm that implies a monolayer of *DNA* molecules. As *Au* nanoparticles are linked together via *DNA* hybridization, electromagnetic coupling between the nanoparticles result in significant damping of their surface Plasmon resonances. The amount of extinction due to scattering is also influenced by the interparticle spacing. Interparticle distance also influences van der Waals and electrostatic forces between the particles, weakly affecting duplex *DNA* stability and hybridization / dehybridization properties.

Can microwaves disrupt the covalent bonds of DNA? The fundamentals of thermodynamics and physics indicate

this is impossible. The majority of these factors have electromagnetic nature. For the spectrum range, where $h\nu << kT$, all the kinds of the biological activity to a certain degree have been already found. The case is somewhat different with the rest of wide range of electromagnetic spectrum, where $h\nu << kT$. This range includes diapasons from the microwaves to infra low frequency. For a long time to infra low frequency range is considered not to influence on alive organisms. The simple physical considerations led for such conclusions: as energy quantum in the spectrum range considerably less, from than the average kinetic energy of molecules ($h\nu << kT$), then infra low frequency absorption in alive tissue may be associated only with the amplification of a molecule rotation, i.e. with the transformation of electromagnetic energy into thermal one [4, 16]. Its studies have demonstrated that microwaves are capable of breaking the covalent bonds of DNA (Fig. 8.).

The exact nature of this phenomenon is not well understood, and no theory currently exists to explain it [4, 17, 19]. Nevertheless, polar molecules are those which possess an uneven charge distribution and respond to an electromagnetic field by rotating. The angular momentum developed by these molecules results in friction with neighboring molecules and converts thereby to linear momentum, the definition of heat in liquids and gases. Because the molecules are forced to rotate first, there is a slight delay between the absorption of microwave energy and the development of linear momentum, or heat. There are some minor secondary effects of microwaves, including ionic conduction, which are negligible in external heating. Microwave heating is, therefore, not identical to external heating, at least at the molecular level, and the existence of a microwave effect is not precluded simply because the macroscopic heating effects of microwaves are indistinguishable from those of external heating.

The change of the resistance (Δ*R*) of the layers from *DNA* polymerized molecules networks (see Fig. 8.) and from *DNA* – linked *Au* nanoparticles in networks [4, 17, 18] on sapphire under rise of the microwave power (*P*) was increased. Resistance of the layer of *DNA* polymerized molecules networks on sapphire increases on $R = 80 \cdot \Omega$ in the range from 0 to $9 \cdot mW$. These changes decrease for this layer after ageing under *UV – VIS* illumination (Fig. 9.). Resistance of the layer from DNA – linked *Au* nanoparticles

in networks on sapphire in the same range increases on $\Delta R = 96 \cdot \Omega$ [4, 17].

The energy level of a microwave photon is only, whereas the energy required to break a covalent bond is $10 \cdot eV$, or a million times greater. Such a behavior the resistance of these layers could be defined by partially breaking part district or changing of the bonds in *DNA* polymerized molecules. There is plenty of evidence to indicate that there are alternate mechanisms for causing *DNA* covalent bond breakage without invoking the energy levels of ionizing radiation. The electrical conductivity of *DNA* was affected with humidity regardless of single or double stranded *DNA* since those measured signals might reflect only the ionic transport. Still, no theory currently exists to explain the phenomenon of *DNA* fragmentation by microwaves although research is ongoing which may elucidate the mechanism. The experiments shows a common pattern – for the first few minutes of irradiation there is no pronounced effect, and then a cascade of microbial destruction occurs. The data pattern greatly resembles the dynamics of a capacitor; first there is an accumulation of energy, and then a catastrophic release. It may simply indicate a threshold temperature has been reached, or it may indicate a two-stage process is at this work.

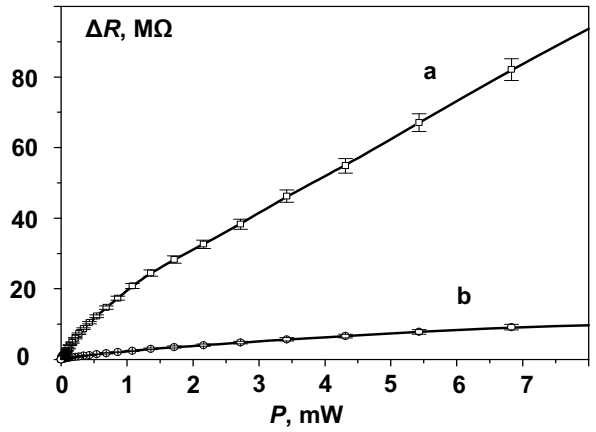

Fig. 8. The change of the resistance (Δ*R*) of the layer from *DNA* polymerised molecules networks on Al_2O_3 (□– points) under microwave power (*P*) and *T* = 300 K [10, 11]. The measurements after temperature cycling (the Δ*R* versus *P*, curve *a*) and after *UV – VIS* spectroscopy (the Δ*R* versus *P*, curve *b*) have been carried out

The second stage of this process may very well be the accumulation of oxygen radicals, which would certainly seem to be primary suspects as they have a considerable propensity for dissociating the covalent bonds of *A*, *C*, *G*, *T* and oxygen radicals can be generated by the disruption of a hydrogen bond on a supermolecule. These molecules exist alongside single *DNA* molecules as "bound" system, two or three layers thick [9]. These molecules share a hydrogen bond with component atoms of the *DNA* backbone, including carbon, nitrogen and other oxygen atoms. At any given point in time one of the hydrogen atoms may be primarily bonded to either an oxygen atom on the supermolecule, or to an oxygen (or other) atom on the *DNA* backbone. The fluctuating character of these shared and exchanged bonds is enhanced by temperature and by the dynamics induced by microwaves. Although the amount of oxygen radicals which may be produced by this process cannot presently be determined, the production of some number of oxygen radicals is inevitable in these circumstances. It must be noted here though, that most of the oxygen radicals produced in this manner would exist only briefly, as they would almost immediately bond to the nearest available site. If this site is an oxygen atom on the *DNA* backbone, I get a covalent bond break, albeit probably only a brief one. The *ac* conductivity measurements of single and double stranded *DNA*s using precision microwave parameter analyzers in the centimeter and millimeter spectral range under different humidity. On the basis of the present results and discussion, the electron transport through a double stranded *DNA* should follow a one-dimensional pathway. However, the double stranded *DNA* molecules in their films were naturally coiled and randomly distributed. They could not be expected to give rise to any electrically conductive signals under this circumstance. Due to extremely high frequencies, the ionic conduction is also negligible. Therefore, these measurements may only reveal the dipole relaxation behavior of solution trapped inside the films in the microwave spectral range. According to the diagram adsorption of solution per nucleotide as a function of humidity in this literature [4, 6, 20], the double and single - stranded *DNA* molecules were identical. This can explain why their *ac* conductivity is identical under that measurement condition. The data about the ac conductivity of the double stranded *DNA* molecules under 0 % and 90 % of relative humidity upon various frequencies suggested that at a high humidity, the ac conductivity of the *DNA* molecules was close to that of water, which is an electrical insulator under a normal condition [1, 18].

The absorbance of *DNA* is the reason radiation can be used the absorbed energy destroys (cause mutations) and kills the organism. When a *DNA* helix is denatured to become single strands, e.g. by heating, the absorbance is increased about 30 percent (see Fig. 9.).

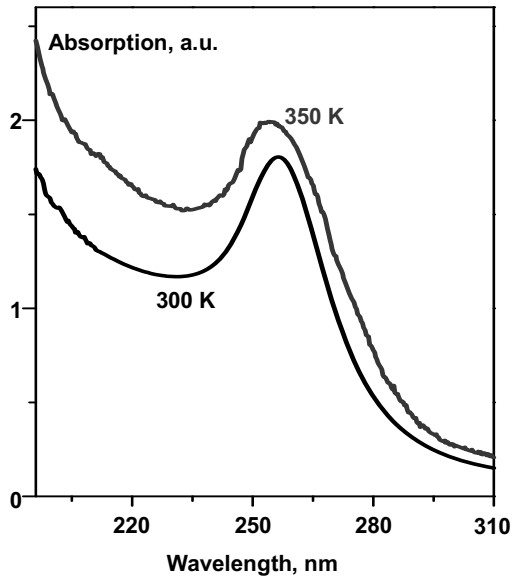

Fig. 9. Absorption in the *UV* spectra of Au / *DNA* nanosystems at two temperatures

Each of the four nucleotide bases has a slightly different absorption spectrum, and the spectrum of *DNA* is the average of them. A pure *DNA* solution appears transparent to the eye, and absorption doesn't become measurable until 320 nm. Moving further into the *UV* region, there is a peak at about 260 nm , followed by a dip between 220 and 230, and then the solution becomes essentially opaque in the far *UV* region. A solution of double stranded, native *DNA*, with a concentration of 0,04 mg/mL has an absorbance of about 1,0 At at the 260 nm peak [6, 19]. This increase, called the

hyperchromic effect, reveals the interaction between the electronic dipoles in the stacked bases of the native helix. Under a high relative humidity, both number and freedom of the water molecules trapped inside the *DNA* films were increased so that the ac conductivity of *DNA* was close to that of water. Although *DNA* tends to repair itself naturally, the simultaneous breakage of a sufficient number of covalent bonds would lead to a catastrophic failure of the entire *DNA* molecule. Due to the exceedingly large number of bonds involved, the matter boils down to a reproducible function of pure probabilities.

The optical properties *Au* nanoparticles are conferred by the interaction of light with electrons on the surface *Au* / *DNA* nanosystems. As an example, the emission spectra for *Au* nanoparticles (Figure 10) are shown. At a specific wavelength (frequency) of light, collective oscillation of electrons on the *Au* nanoparticle surface cause a phenomenon called surface Plasmon resonance resulting in strong extinction of light. The particular wavelength, or frequency, of light where this occurs is strongly dependant on the *Au* nanoparticle size, shape, and surface, and agglomeration state as described. The intensive absorption by all of the nucleotides in the *UV* range is almost entirely determined by purine and pyridine bases. The interaction of the four nucleotide bases causes electronic perturbations in the complexes. When incorporated into *DNA* duplexes, *G* and *C* are able to be oxidized by excited-state 2-aminopurine (*Ap*). Since the reaction of the excited state of *Ap* with the base analog in sine (*I*) is not thermodynamically favorable, charge transfer between *G* or *C* and photo excited *Ap* can be evaluated using inside containing duplexes as references [1, 4, 14].

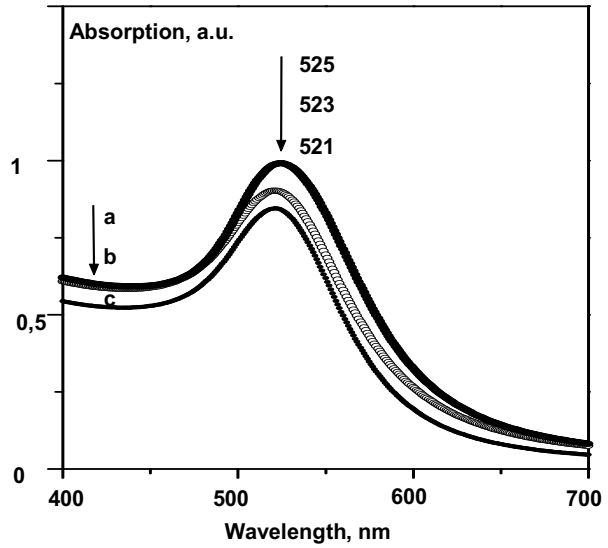

Fig. 10. Absorption spectra separated *Au* nanoparticles – negative charged citrate – capped colloid *Au* particles in water solution with sizes in diameters 8,8 nm, 10,5 nm, 16,7 nm – curves *a, b, c*, correspondingly. [6]

Further, because duplexes containing *C* differ from those containing *G* by only one atom, the effect of driving force on DNA - mediated charge transfer behavior may be examined without drastically altering the structure of the assemblies. Fixing the *Au* nanoparticles at specific sites eliminates the distribution of distances usually present when charge transfer is examined with intercalators tethered to the end of *DNA*. These perturbations can be observed through emission studies and spectroscopic titration. The emission spectra for these bases were similar Density of states for the *Au* nanoparticles in 2D - plates from *Au* / DNA nanosystems and *I* - *V* characteristics gap - *Au* nanoparticle hosted in 2D - plate from *Au* / DNA - sapphire substrate for different *Au* nanoparticles sizes (A, B, C). It emits in a buffer at room temperature with a maximum at 523 nm. The obtained results can be used for the analysis of an optical response of systems containing DNA's nucleotides and *Au* nanoparticles [1, 4, 10].

The influence of *Au* nanoparticle size on the surface plasmon resonance is illustrated in Figure 11, where the absorption maximum (lambda max) increases from 448 nm to 456 nm for diagnostics sizes in range at $5 \div 100$ nm spherical *Au* nanoparticles, respectively. As a comparison *Au* nanoparticles of sizes below 2 nm do not exhibit surface Plasmon resonance [2, 4, 11].

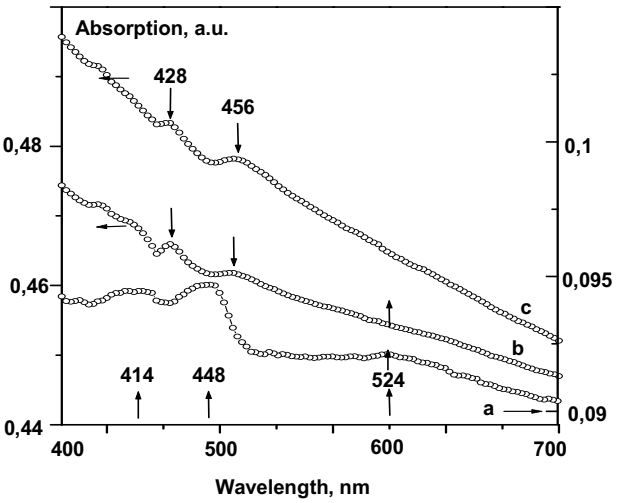

Fig. 11. Absorption spectra of *Au* nanoparticles: a – in 2D – plates into gel without *DNA*; *b*, *c* – in *Au* / *DNA* nanosystems in 2D - plates into gel with mixture of 2D – plates, having sizes in big side 100÷150 nm (*b*) and 8÷25 nm (*c*)

A major determinant of the optical properties of *Au* nanoparticles is their shape. By synthesizing *Au* nanoparticles of different shapes, the surface Plasmon resonance can be easily be tuned to give absorption maxima from around 500 nm into the near-infrared part of the spectrum. The difference in absorption properties between spherical and irregular-shaped *Au* nanoparticles of the same average size is caused by an anisotropic distribution of the surface electron layers. It's the transmission spectra of *Au* / *DNA* nanosystems in 2D - plates (*a*) and *DNA* molecules (*b*) in adsorbed layers from gels on dielectric substrate (Fig. 12). *IR* spectra of the adsorbed layers from these gels on dielectric substrate in the range of $800 \div 1500$ cm^{-1} at $T = 300$ K. The surface Plasmon resonance of the *Au* particles coupled by DNA chains are recorded and compared with the spectra of isolated particles. Upon adding linker DNA, the DNA hybridization leads to aggregation of gold nanoparticles, as demonstrated in the *Au* surface Plasmon peak (520 nm) shift of the *DNA* – modified *Au* nanoparticles. In the cases of *DNA* chains functionalized with two thiol groups the spectra shows a broadening and a red shift of the surface plasmons which is a result of coupling the particles by this chains. The aggregation starts with the wavelength shift of the Plasmon band, followed by broadening and more shifting of the peak as hybridization continues. These results indicate that the initial aggregation takes place with increasing volume fraction, followed by increasing network size [4, 6].

The next act measurements have in direct measurement a single *DNA*. The result decreasing It's the energy barrier between cluster and sonde will also decrease barrier characteristics *DNA* oligomers. The cluster level structure might change when compared to the corresponding free system. As is clear from Figure 3 and Figure 13, the *DNA* oligomers does not conduct charge for voltage below about 0,2 V at room temperature. DNA molecules on a sapphire surface between two gold electrodes about 3 μm, also showed a resistance of 10 TΩ (see Fig. 13). For instance, poly(d*G*) – poly(d*C*)*DNA* with no thiol groups showed resistances greater than 1 TΩ on both sapphire substrates. The *I* – *V* characteristics for poly(d*A*) – poly(d*T*) *DNA* showed a large bandgap at temperatures lower than 150 K. This can be accounted for by a small polaron hopping model [4, 10], where the current is given by $I \propto \sinh bV \exp[-Ea / k_bT]$, where E_a is the activation energy, *T* is the background temperature, $b = ea / 2k_BTd$, e is the electron charge, a is the hopping distance, and d is the distance between the electrodes. The details of the cluster - sonde interaction will determine the changes in geometrical and electronic properties with respect to the unsupported case. Equation describes the *I* – *V* characteristics of poly(d*A*) – poly(d*T*) DNA very well if b is taken to be independent of temperature. Furthermore, poly(d*G*) – poly(d*C*) DNA shows temperature dependence of the current down to 20 K and seems to have two molecular vibration frequencies which contribute to the polaron motion, whereas poly(d*A*) – poly(d*T*) DNA shows temperature dependence only down to 50 K and seems to support only one molecular vibration. When a transverse microwave field is applied, the potential along the DNA chain will be adjusted due to the special structure of a DNA double helix. This modulation changes the electronic structure of the DNA molecule and further influences its transport property. The transverse electric field will suppress the current through the device. The reason is that the transverse electric field potential tends to make the on-site energy of the poly(*G*) - poly(*C*) DNA molecule into a "disorder". This "disorder" changes the wave-function of the electron and further influences conductivity. The calculation reveals that the suppression on the current is also related to the direction of the transverse electric field, which is denoted by phase φ_0, as shown in Fig. 6. Since the modulation is harmonic due to the double helix structure of DNA molecule, choose the phase $\varphi_0 = 0$ to correspond to the direction that the transverse electric field points to from base *G* to base *C* of the first base pair. The modulated potential along a one-helix-period ploy(*G*) - poly(*C*) *DNA G* and *C* chain is for phase $\varphi_0 = 0$ and $\varphi_0 = \mathrm{p}$. At a fixed strength of the transverse electric field the amplitude of the "disorder" is unchanged, but different directions change the shape of the modulation in detail, which will make a difference of the conductance. Fig. 13 shows the dependence of the current on φ_0 for different strengths of the transverse electric field for a simple Au / DNA / Au device. The straight solid line corresponds to the case when the transverse electric field is absent. When the transverse electric field is turned on, the current has fluctuating behavior with φ_0. With a larger transverse electric field fluctuation becomes more notable. Measurements at both ambient conditions and in a vacuum were performed, with no substantial change in the results.

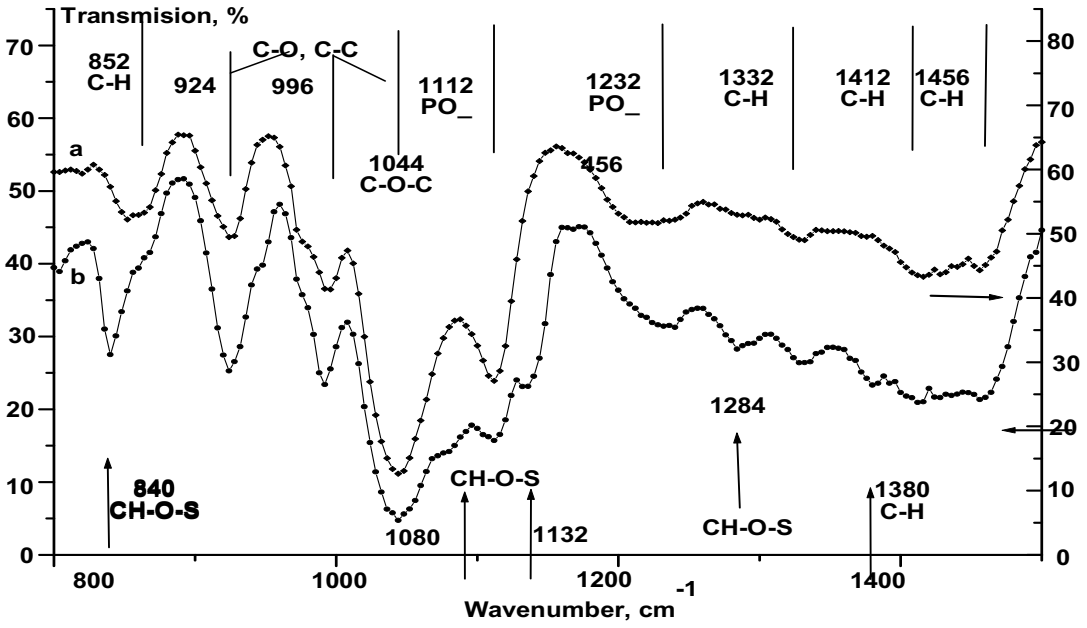

Fig. 12. The transmission spectra of *Au* / *DNA* nanosystems in 2D – plates (*a*) and *DNA* molecules (*b*) in adsorbed layers from gels on sapphire substrate

In the *I* – *V* curves threshold voltages to showing the inclusion of backbones opens a gap between the HOMO and the lowest unoccupied molecular orbital. For sufficiently high applied voltages, as can be observed for almost all models for the voltage range depicted in Figure 13. Next, a non-periodic sequence of base pairs can drastically suppress the currents to the *DNA* sequence. This strong suppression is do not show a large suppression at such short lengths *DNA*, while longes already exhibit a several orders of magnitude drop in current. There are steps appearing in some *I* – *V* curves, which are due to resonances in the transmission probabilities. Such resonances are more relevant and robust in the telemetric sequences. Resonance effects are still present in some cases for disordered short sequences, but they do not last for longer systems, as can be systematically appreciated in Figure 14. The complexity of the DNA systems does not as yet a definitive conclusion to be drawn on the mechanisms

leading to sequences on *I – V* characteristics. Nevertheless, the consistency among the results found here for different measurement, widely discussed in the literature [2, 4, 11], suggests that important qualitative physical and chemical aspects have been captured in the present work. These steps are enhanced and not washed out by adding parallel chains, irrespective of the starting points defined at the interface of each sequence with the contact. The drastic difference in the lengths dependence of the current for *DNA* will allow for better comparison and interpretation of experimental data.

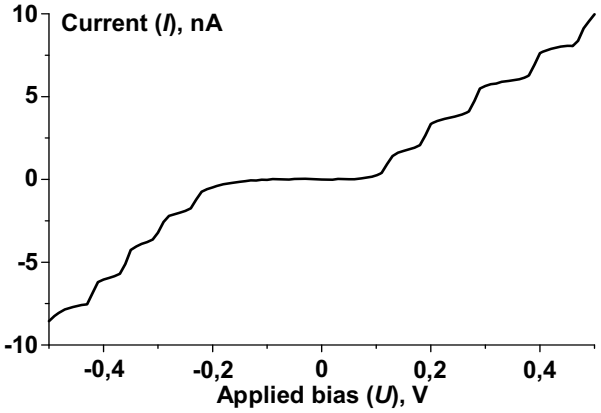

Fig. 13. I – V characteristics is placed across single the DNA molecule. The inset shows the current versus the gate voltage at a source-drain voltage of 0.5 V. Reprinted with permission from [21]

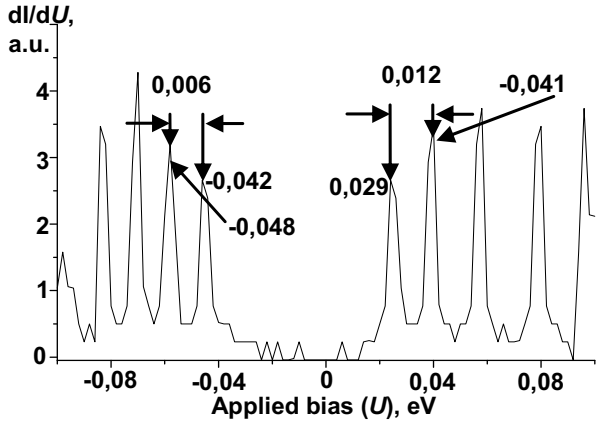

Fig. 14. The differential conductivity – voltage characteristics of is placed across single the *DNA* molecule

Conclusions. *DNA* molecules as building blocks in nanotechnology of nanosystems has probably only just begun, but already produced some striking results as in electronic, optic nanosystems engineering such as in tissue engineering. The first step on this way is the study of *DNA* on the molecular level, which may point to new directions in nanosystems design and construction – not just biomolecular systems, but actually using *DNA* biomolecules themselves to construct novel nanosystems. Among the variety of approaches to *DNA* - based supramolecular physic, the strategy of replacing *DNA* natural bases by alternative bases that possess distinct shape, size, or function has allowed the modification of *DNA* in a highly specific and site selective manner. This approach is replacing bases *DNA* on *Au* cluster restricted to molecules with shapes and sizes that are commensurate to normal bases to ensure that the *DNA* modifications occur highly specifically and site selectively. The new generation of such nucleoside mimics was found in which the hydrogen bonding interactions were replaced by metal-mediated base pairing. The advantage of this modification strategy is that it allows the metal ions to be replaced in the interior of the *DNA* duplex.

The geometrical properties and electronic structure of single *DNA* nucleosides (d*A*, d*T*, d*G*, d*C*) adsorbed on a metallic surface of *Au* cluster are determined. I investigate multiple adsorption geometries and the resulting molecule surface interaction mechanisms self-assembly *DNA – Au* nanosystems. For *A*, I found negligible differences between the binding energy in the two configurations investigated, while for *G* this difference reaches the maximum value among the four nucleosides (i.e., 0.79 eV). The projected density of states indicates that the physisorption is the main cause of the binding energy. Nevertheless, for the adsorbed d*C*, point out the presence of the chemical interaction too. While the absolute values of the molecule surface charge transfer are small, they are qualitatively dependent on the orientation of the nucleosides to the surface. If the *DNA* bases are oriented perpendicular to the surface, the electronic population of molecules decreases, while the parallel orientation of the *DNA* bases with respect to metal surface leads to an increase of electronic population on the molecules.

The laboratory models investigated in this work - based on the naturally occurring, physisorption stable threads - should provide ideal benchmark situations for systematic investigations of *DNA* electronic transport, as well as for the development of *DNA*-based molecular nanoelectronic applications using *Au* as contacts. In particular, the *I – V* characteristics presented here show promise of a wide range of interesting nanocircuitry on complex patterns of hollowed thin films on substrates sapphire bridged by DNA sequences. The *I - V* curves suggest the existence of stepped structures smal independent of length and sequencing initialisation at the self-assembly *DNA – Au* nanosystems. They are present independent of lengths and sequence initialisation at the *Au* contacts. Surely, the molecule-electrode coupling can drastically influence the magnitude and fluctuations of the current.

The *ac* impedance spectroscopy provides further evidences for the electrical conductivity of double stranded DNA. The spectra images of *DNA* build up a proportional relationship of *DNA* electrical conductivity and the number of the *DNA* molecules stretched over the gap *Au* electrodes. The enzymes DNA was used to degrade the *DNA* molecules stretched across the electrode gaps, which results in a significant increase in the charge-transfer resistances. These impedance spectra do not demonstrate any feature of ionic conduction and small sensitivity to light. The spectra do not support *DNA* as metallically conductive molecules, which should give a constant resistance on the real resistant axis of an impedance spectrum. Instead, they suggest the double stranded DNA to be a semiconductor. Different from some semiconductors, such as silicon, the *DNA* conductivity should follow the mechanism of one-dimensional electron transport through the π stack of double stranded *DNA* base pairs.

Reference

1. Cancer and aging as consequences of un-repaired DNA damage. In: New Research on DNA Damage / Ed. by Honoka Kimura, Aoi Suzuki. – NewYork., 2008. 2. Frontiers of nano-optoelectronic systems / Ed. by L. Pavesi, E. Busaneva. – Dordrecht., 2000. 3. Future Trends in Microelectronics. Up the Nano Creek / Ed. by S. Luryi,, Xu J., A. Zaslavsky. – NewYork., 2007. 4. Nano and Molecular electronics: handbook / Ed. by S.E. Lyshevski. – Boca Raton, 2007. 5. Nanotechnology: an Introduction to Nanostructuring Techniques / Ed. by M. Kohler, W. Fritzsche. – NewYork., 2007. 6. Optical spectroscopy of semiconductor nanostructures / Ed. by E.L. Ivchenko. – Harrow., 2005. 7. Self-assembled nanostructures / Ed. by J.Z. Zhang, Z.L. Wang , J. Liu et al. – New York., 2004. 8. Springer Handbook of Nanotechnology / Ed. by B. Bhushan. – Berlin., 2004. 9. Ivanyuta O., Tsamis C., Scharff P. et al, Design and study of DNA/nanocarbon and macrocyclic metal complex/C60 nanostructures // In

Work Book of NATO ARW, Frontiers in molecular-scale science and technology of nanocarbon, nanosilicon and biopolymer integrated nanosystems, Ilmenau – 2003. 10. Ivanyuta O., Tsamis C., Scharff P. et al, DNA, DNA/metal nanoparticles, DNA/nanocarbon and macrocyclic metal complex/fullerene molecular building blocks for nanosystems: electronics and sensing //In Book Frontiers of multifunctional integrated nanosystems, Ed. by Buzaneva E, Scharff P., NATO Science Series II, Mathematics, Physics and Chemistry – NAII. Dordrecht. – 2004. – Vol 152. – P. 251–276. 11. Andersen ES, Dong M, Nielsen M., Self-assembly of a nanoscale DNA box with a controllable lid. // Nature – 2009 – Vol. 459 – P. 7243. 12. Aldaye FA, Palmer AL, Sleiman H.,F Assembling materials with DNA as the guide. // Science. – 2008. –Vol 321, – P. 5897. 13. Bogdan D., Morari C., Electronic Properties of DNA Nucleosides Adsorbed on a Au(100) Surface. // J. Phys. Chem. C. – 2012. – Vol. 116 (13). – P. 7351–7359. 14. Calborean A., Buimaga-Larinca L., DFT simulation of vibrational properties of adenine adsorbed on gold surface: The effect of periodic boundary conditions // Computational and Theoretical Chemistry. – 2012. – Vol. 993. – P. 106–112. 15. Hughes-Stamm S.R., Ashton K.J., Daal A., Assessment of DNA degradation and the genotyping success of highly degraded samples. // Int. J. Legal Med. – 2011. – Vol. 125(3). – P. 341–348. 16. Isaksson J., Acharya S, Barman J, et.al., Single-stranded adenine-rich DNA and RNA retain structural characteristics of their respective double-stranded conformations and show directional differences in stacking pattern. // Biochemistry. – 2004. – Vol. 43(51). – P. 15996–6010. 17. Ivanyuta A.N., Prokopenko O.V. Sensing of DNA polymerised molecules in networks // In Proceedings of PLMMP-2010 5th International Conference Physics of Liquid Matter: Modern Problems. – 2010. 18. Ivanyuta O., Gobsh G., Scharff P. et al., Photonics of mimetic biomolecules: the photoluminescence spectroscopy of cysteine molecules in thin layer // In Proceedings of the VI International Conference on Electronics and Applied Physics. – 2010. 19. Rosa M., Corni S, Di Felice R., A Density Functional Theory Study of Cytosine on Au(111) // J. Physical Chemistry. – 2012 . – Vol. 116(40). – P. 21366–21373. 20. Sun W., Di Felice R., Nature of the Interaction between Natural and Size-Expanded Guanine with Gold Clusters: A Density Functional Theory Study. // J. Physical Chemistry. – 2012. – Vol. 116(40). – in print. 21. Watanabe H., Manabe C., Shigematsu T et al., Single molecule DNA device measured with triple-probe atomic force microscope // Appl. Phys. Lett. – 2001. – Vol 79. – P. 2462–2465.

Submitted on 20.11.12

О. Іванюта, канд. фіз.-мат. наук,
каф. електрофізики, радіофізичний факультет,
КНУ імені Тараса Шевченка, Київ

ЕЛЕКТРОФІЗИЧНІ ВЛАСТИВОСТІ *ДНК* І *ДНК*: *AU* МОЛЕКУЛЯРНИХ КЛАСТЕРІВ НА САПФІРІ

Покриття ДНК, ДНК: Au, як кластери з гелієвих розчинів можуть виявляти магнітну й електричну активність у біосенсорній системі та виявити функціональні властивості для мікрохвильової техніки. Дослідження було зосереджено на аналізі їх ВАХ та спектрів методами розпізнавання і прогнозування цих молекулярних взаємодій на основі їх первинної структури та взаємозв'язку з фізико-хімічними властивостями. Результати показали, що ці молекулярні шари кластерів на підкладках Al_2O_3 можуть проводити електричний струм і реагувати на потужність НВЧ.

Ключові слова: ДНК, UV-VIS-NIR спектри, точкове джерело низько енергетичних електронів, вольт-амперна характеристика.

А. Иванюта , канд. физ.-мат. наук,
каф. электрофизики, радиофизический факультет,
КНУ имени Тараса Шевченко, Киев

ЭЛЕКТРОФИЗИЧЕСКИЕ СВОЙСТВА *ДНК* И *ДНК*: *AU* МОЛЕКУЛЯРНЫХ КЛАСТЕРОВ НА САПФИРЕ.

Покрытие ДНК , ДНК:Au, как кластеры с гелиевых растворов могут проявлять магнитную и электрическую активность в биосенсорной системе и функциональные свойства для микроволновой техники. Исследование было сосредоточено на анализе их ВАХ и спектров методами распознавания и прогнозирования этих взаимодействий на основе их первичной структуры и взаимосвязи с физико - химическими свойствами. Результаты показали, что эти молекулярные слои кластеров на подложке Al_2O_3 могут проводить электрический ток и реагировать на мощность СВЧ.

Ключевые слова: ДНК, UV-VIS-NIR спектры, точечный источник низко энергетических электронов, вольт-амперная характеристика.

UDC 577.3

K. Karpenko, post grad. stud., O. Sudakov, Ph.D., Department Medical Radio Physics,
Faculty of Radio Physics, Taras Shevchenko National University of Kyiv

INFLUENCE OF RECOVERY MODEL PARAMETERS ON SYNCHRONIZATION IN NEURAL CORTICAL STRUCTURE DURING DESCENDING INFORMATION TRANSFER

Neurons interaction in networks with complex dynamics was investigated, the synchronization phenomenon for descending information process in cortical column was considered. The synchronization coefficient dependency on different variations of Izhikevich model parameters is depicted on corresponding plots. Visual study of network synchronization is performed by means of raster plots. Synchronization coefficients on different layers of cortical column were compared. Proved that time-scale parameter of membrane potential recovery variable has the weakest influence on network synchronization.

Keywords: synchronization coefficient, Izhikevich model, cortical network, descending information process.

Problem statement. Last years studies of brain neuron networks and principles of information presentation and transformation in the brain are of great interest. Today number of tools and resources for neurophysiological experiments allows us to get more information about functioning of different brain neuron networks. One of the main directions in this science brunch is development of physical and mathematical neuron models that describe basic functional possibilities of neurons and convenient for theoretical researches. Such models are very popular in neurons researching to solve one of the main neurophysiological and biophysical problems: determination how information flows in the network is related to network's topology.

Analysis of recent researches and publications. Active researches of brain's structural organization summarized that the main principle of brain's organizing is the modularized structure and partial information processing. [8] Neocortex is responsible for thinking, speaking and other processes of nervous system and has the most representative modularized organization. Aggregation of cells and links in the cortex into horizontal layers may lead to the conclusion that main interactions in the brain take place in the horizontal planes. But in the 1930-s Spanish scientist Rafael Lorente de No [7, 6] first supposed that cortical processes are local and take place in the vertical columns. Lorente de No assumed that neurons in such structures are associated into closed networks with ring topology. It must be mentioned that till nowadays scientists have no consensus about cortical column's form (cylinder, cone, line, ensemble, "barrel" and others) [9, 10]. Nevertheless comparison of results from different functional researches shows the existence of vertical neuron groups. Hebb [4] hypothesized that neurons ensemble is organized as 3d network consisted of elements with different functional states. Synaptic currents in such network amplify each other by synchronous occurrences. Since the beginning of 60 years this point of